STIFFNESS HISTORY OF ASPHALT CONCRETE SURFACES IN ROADS

Mohamed Y. Shahin and B. Frank McCullough, Center for Highway Research, University of Texas at Austin

A system for predicting the stiffness history of an asphalt concrete pavement layer throughout its design analysis period has been developed. The system uses standard material properties and environmental inputs to predict the daily changes in stiffness due to temperature variations and also the long-term changes in stiffness due to hardening of the asphalt cement binder. This system was developed as part of an overall system for the prediction of low-temperature and thermal-fatigue cracking in flexible pavements. The following procedures and models were developed from actual projects and other research results: models to estimate the asphalt concrete stiffness from the ordinary laboratory measurements, procedure to estimate the loading time for temperature, and models to predict the in-service aging of asphalts. The system has been used in predicting low-temperature and thermal-fatigue cracking and has shown a good degree of reliability.

•PROPER estimation of asphalt concrete stiffness is essential for calculating thermal stresses and fatigue distress due to traffic loading and temperature cycling and for determining flexible pavement design in general. If the stiffness is too low, load distress may develop; if it is too high, temperature cracks are likely to occur. The calculation of thermal stresses and fatigue distress in flexible pavements demands the estimation of many values of asphalt concrete stiffness at many temperatures. For example, the calculation of thermal stresses on an hourly basis for a single year will demand the estimation of 8,640 (360 × 24) stiffness values. Therefore, the model for estimating the asphalt concrete stiffness should be in a form that can be programmed.

It is an established fact that asphalt concrete is neither elastic nor viscous but viscoelastic; i.e., its stiffness is a function of temperature and loading time. Moreover, the aging of asphalt adds an important dimension to the stiffness of the asphalt concrete. In this research effort, a system for estimating the asphalt concrete stiffness as a function of temperature, loading time, and age has been developed. The following are the constituents of the system:

1. Models to estimate the asphalt concrete stiffness from the ordinary laboratory measurements,
2. Procedure to estimate the loading time for temperature, and
3. Models to predict the in-service aging of asphalts.

The system has been used in predicting low-temperature and thermal-fatigue cracking (1) and has shown a good degree of reliability.

ASPHALT CONCRETE STIFFNESS

There are three approaches to characterizing the behavior of viscoelastic materials: models, direct measurements, and indirect measurements. The last approach is utilized here in estimating asphalt concrete stiffness. This choice is based on the belief

Publication of this paper sponsored by Committee on Flexible Pavement Design.

that Van der Poel's method (2) can be computerized to fit in the overall system for predicting the history of the asphalt concrete stiffness.

Several investigators have investigated the accuracy of the Van der Poel and Heukelom and Klomp nomographs. Pell and McCarthy (3) reported that the general stiffnesses computed by Van der Poel compared reasonably well with those measured on actual samples. Monismith (4) also checked laboratory-determined stiffness values with both laboratory compacted samples and samples cut from in-service pavements. The results showed reasonable agreement with those determined from Heukelom and Klomp.

Van der Poel (2) also independently checked the accuracy of his nomograph and concluded that the difference in measured stiffness values of an asphalt and the stiffness obtained from the nomograph seldom exceeded a factor of 2.

The concept of stiffness was introduced by Van der Poel (2) as follows:

$$\text{Stiffness modulus (S)} = \frac{\text{tensile stress}}{\text{total strain}} \tag{1}$$

The nomograph for estimating the asphalt stiffness was derived by Van der Poel from experimental data from two types of tests: constant stress (static creep test in tension) and dynamic test with an alternating stress of constant amplitude and frequency.

Van der Poel's nomograph was modified slightly by Heukelom and Klomp (5), in that the stiffness is determined in kg/cm^2 instead of N/m^3, and the lines for negative penetration indexes are in a different location. This modified nomograph is shown in Figure 1. The determination of the asphalt stiffness from the nomographs published by Van der Poel and Heukelom and Klomp requires three parameters: loading time, test temperature minus softening-point temperature, and penetration index of the asphalt.

The stiffness of the asphalt concrete mixture depends on the stiffness of the asphalt and the volume concentration of the aggregate. Heukelom and Klomp gave the following equation to estimate the stiffness of the asphalt concrete when the stiffness of the asphalt cement is determined from their nomograph (Fig. 1):

$$S_{mix} = S_{ac}\left[1.0 + \left(\frac{2.5}{n}\right)\left(\frac{C_v}{1.0 - C_v}\right)\right]^n \tag{2}$$

where

$$n = 0.83 \log_{10}\left(\frac{4 \times 10^5}{S_{ac}}\right);$$

S_{mix} = stiffness of asphalt concrete mixture, kg/cm^2;
S_{ac} = stiffness of asphalt cement, kg/cm^2; and
cv = volume concentration of the aggregate.

The volume concentration of the aggregate in a mixture is defined as follows:

$$C_v = \frac{\text{volume of compacted aggregate}}{\text{volume of (asphalt + aggregate)}} \tag{3}$$

This equation can be substituted by an equivalent equation (Eq. 4) by replacing the terms with values that can be measured on an asphaltic concrete core cut from a pavement or a compacted laboratory sample.

$$C_v = \frac{1}{1 + C} \tag{4}$$

Figure 1. Nomograph for predicting the stiffness modulus of asphaltic bitumens (5).

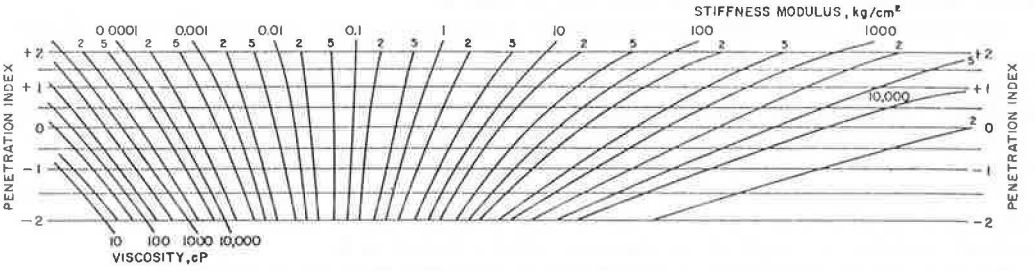

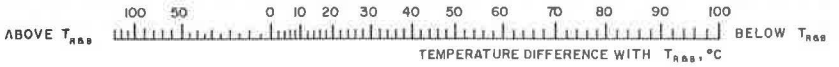

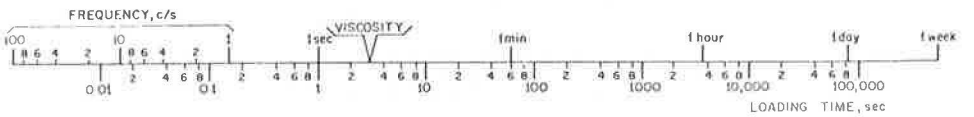

where

$$C = \left(\frac{W_a}{W_g}\right) \times \left(\frac{G_g}{G_a}\right) = (\text{percentage of asphalt by weight of aggregate}/100)\left(\frac{G_g}{G_a}\right),$$

W_a = weight of asphalt,
W_g = weight of aggregate,
G_a = specific gravity of asphalt, and
G_g = specific gravity of aggregate.

The relation shown in Eq. 2 is applicable to well-compacted mixtures with about 3 percent air voids. For mixtures with air voids greater than 3 percent, Draat and Sommer (6) derived a correction to be applied to the C_v:

$$C_v' = \frac{C_v}{1 + H} \tag{5}$$

where H = actual air voids - 0.03.

After a review of the literature and also personal contact with Van der Poel, it was found that no equation has been developed since the nomograph was first published in 1954. As a result, a predictive mode was developed through the use of regression methods. The method selected was the stepwise regression because it was felt that this method provides the best selection of independent variables. The dependent variable was chosen as the $\log_{10}$ of stiffness because the stiffness varies over many orders of magnitude. The independent variables selected were loading time t, temperature of test minus softening-point temperature T, penetration index PI, log t, log T + 101, log PI + 3, t^2, T^2, PI^2, t^3, T^3, PI^3, all two-way interactions of these variables, and other combinations of these factors that seemed theoretically reasonable.

As explained in Draper and Smith (7), the stepwise regression procedure starts with the simple correlation matrix and enters into regression the independent variable X most highly correlated with the dependent variable Y, $\log_{10}$ (stiffness). Using partial correlation coefficients, it then selects as the next variable to enter regression that X-variable whose partial correlation with the response Y is highest, and so on. The procedure reexamines "at every stage of the regression the variables incorporated into the model in previous stages" (7). The program does this by testing every variable at each stage as if it had entered last.

The overall goals for the prediction equation were as follows:

1. The final equation should explain a high percentage of the total variation ($R^2 \geq 0.98$),
2. The standard error of the estimate should be less than 0.20 (this value being a log) to ensure a small coefficient of variation,
3. All estimated coefficients should be statistically significant with $\alpha \leq 0.05$, and
4. There should be no discernible patterns in the residuals.

An attempt to characterize the entire nomograph with a single regression equation was first made. A large factorial grouping of data as shown in Figure 2 was taken from the nomograph in Figure 1. The data represent loading time from 10^{-2} to 10^{-5} sec, PI from -2 to +2, and $T_{test} - T_{R\&B}$ from +50 to -100 C. After many attempts to obtain a suitable prediction equation that met the goals listed, and after not being able to reduce the standard error of the estimate to an acceptable level, we decided to split the nomograph into two parts and fit a separate equation to each part. Almost all of the stiffness values of practical significance to a pavement design engineer are greater than the 10 kg/cm^2 of the asphalt cement. This is approximately 400 kg/cm^2 for a mix with C_v of 0.86, which equals about 5,700 psi. Therefore, a regression equation was derived using the data shown in Figure 2 with stiffness values less than 10 kg/cm^2, and another regression equation was built using all data that had stiffness values greater than 10 kg/cm^2. Acceptable prediction equations were then obtained for each portion of the data that met all of the goals set for the regression equations.

The following equations were obtained with the corresponding statistics:

1. For a stiffness value of 10^{-7} to 10^{1} kg/cm^2, the prediction model is

$$\log_{10} S = -1.35927 - 0.06743(T) - 0.90251 \log(t) + 0.00038(T^2) - 0.00138(T \times \log t) + 0.00661(PI \times T) \quad (6)$$

where

T = test temperature minus softening-point temperature, deg C;
t = loading time, sec; and
PI = penetration index.

The corresponding statistics are $R^2 = 0.99$, standard error of estimate = 0.1616, and n = 126 data points. The range of factors is PI = -2 to +2, T = +50 to -100 C, and t = 10^{-2} to 10^{5} sec.

2. For a stiffness value of 10 to 20,000 kg/cm^2, the prediction is

$$\log_{10} S = -1.90072 - 0.11485(T) - 0.38423(PI) - 0.94259 \log(t) - 0.00879(T \times \log t) - 0.05643(PI \times \log t) - 0.02915(\log t)^2 - 0.51837 \times 10^{-3}(T^2) + 0.00113(PI^3 \times T) - 0.01403(PI^3 \times T^3) \times 10^{-5} \quad (7)$$

The corresponding statistics are $R^2 = 0.98$, standard error of estimate = 0.1638, and n = 79 data points. The range of factors is PI = -1.5 to +2.0, T = +50 to -100 C, and t = 10^{-2} to 10^{5} sec.

The models were verified by plotting the stiffness values obtained from the nomograph against the stiffness as calculated from Eqs. 6 and 7. The results shown in Figures 3 and 4 indicate that the models are reliable.

The following guidelines are given for using the equations to predict asphalt stiffness:

1. Use Eq. 6 only to predict stiffness from 10^{-7} to 10 kg/cm^2, and use Eq. 7 only to predict stiffness from 10 to 2×10^{4} kg/cm^2. The user should not employ predictions that fall outside of these limits.
2. The ranges given for T, t, and PI should not be exceeded. It was found that Eq. 7 values of stiffness obtained when the PI was -2 were not accurate enough, so use of the equation is limited to a PI of -1.5 or greater.

Equations 6 and 7 can be used to estimate the asphalt concrete stiffness using Eq. 2.

LOADING TIME FOR ESTIMATING ASPHALT STIFFNESS

Asphalt stiffness is partly dependent on the loading time. For traffic, the loading time can be physically measured or estimated; so far as temperature is concerned, the thermal loading time has been a question to be answered by engineering judgment. Most engineers have considered the thermal loading time as the time corresponding to the temperature interval, ΔT (Eq. 8), used for calculating the thermal stresses.

Although this may seem logical initially, it does not appear that it actually is. Instead, thermal loading time is fictitious and depends mainly on the rate of temperature drop and the asphalt concrete mixture properties. This can be shown by using the experimental work performed by Monismith et al. (8). In this experiment, an asphalt concrete beam was subjected to a temperature drop, and the developed thermal stresses were measured. The properties of the mixture are given in Table 1.

The specimens were subjected to a temperature drop from 75 to 35 F. The calculations were simplified by assuming the temperature drop to be linear (Fig. 5). A factorial experiment was then designed for the estimation of thermal stresses under different loading times and temperature intervals (Fig. 6). Equation 8, after Hills and Brien (9), was used for the calculations:

Figure 2. Factorial data obtained from nomograph (5) (in kg/cm^2).

Loading Time, seconds / Penetration Index of Asphalt / T test - TRB, °C		10^{-2}	10^{-1}	10^{0}	10^{1}	10^{2}	10^{3}	10^{4}	10^{5}
+50	-2	3.3E-3	4.0E-4	4.2E-5	5.0E-6	4.0E-7	7.0E-8	1.0E-8	1.0E-9
	-1	7.2E-3	9.5E-4	1.0E-4	1.1E-5	9.5E-7	1.0E-7	1.8E-8	2.0E-9
	0	1.3E-2	1.7E-3	2.0E-4	2.1E-5	2.0E-6	2.3E-7	3.0E-8	5.1E-9
	+1	2.0E-2	2.8E-3	4.0E-4	4.4E-5	4.0E-6	5.0E-7	5.1E-8	7.1E-9
	+2	2.7E-2	4.2E-3	5.7E-4	7.7E-5	5.5E-6	1.0E-6	6.1E-8	1.0E-8
+20	-2	1.3E-1	1.6E-2	1.8E-3	1.8E-4	1.8E-5	1.9E-6	1.9E-7	4.1E-8
	-1	2.0E-1	2.3E-2	2.9E-3	2.9E-4	3.0E-5	2.9E-6	2.9E-7	5.1E-8
	0	2.3E-1	3.0E-2	3.8E-3	4.1E-4	4.6E-5	5.0E-6	4.7E-7	7.1E-8
	+1	2.4E-1	3.5E-2	4.9E-3	5.7E-4	7.2E-5	7.0E-6	6.5E-7	1.0E-7
	+2	2.4E-1	4.1E-2	6.0E-3	8.5E-4	1.1E-4	1.1E-5	1.0E-6	2.0E-7
-10	-2	3.0E1	3.7E0	4.0E-1	4.4E-2	3.9E-3	4.6E-4	5.0E-5	5.0E-6
	-1	1.4E1	2.0E0	2.8E-1	3.4E-2	3.4E-3	4.0E-4	4.2E-5	4.6E-6
	0	7.7E0	1.4E0	2.2E-1	3.0E-2	3.0E-3	3.8E-4	4.2E-5	4.6E-6
	+1	5.0E0	1.1E0	1.9E-1	2.6E-2	2.9E-3	4.0E-4	5.0E-5	4.7E-6
	+2	4.0E0	9.0E-1	1.6E-1	2.4E-2	3.0E-3	4.6E-4	6.0E-5	5.0E-6
-40	-2	1.2E4	5.0E3	1.4E3	2.2E2	2.2E1	2.5E0	3.5E-1	3.7E-2
	-1	1.7E3	5.7E2	1.9E2	3.8E1	4.9E0	6.0E-1	8.0E-2	8.5E-3
	0	5.7E2	2.1E2	6.0E1	1.1E1	1.9E0	2.5E-1	4.0E-2	4.5E-3
	+1	2.5E2	8.5E1	2.5E1	4.9E0	1.0E0	1.6E-1	2.3E-2	3.0E-3
	+2	1.02E2	3.9E1	1.15E1	3.2E0	6.0E-1	1.1E-1	1.7E-2	2.0E-3
-70	-2	2.6E4	2.3E4	2.0E4	1.8E4	1.7E4	1.3E4	5.6E3	1.4E3
	-1	2.0E4	1.6E4	1.2E4	6.7E3	2.4E3	1.0E3	3.0E2	7.0E1
	0	1.1E4	7.0E3	3.7E3	1.6E3	6.0E2	2.3E2	6.2E1	1.1E1
	+1	5.1E3	2.3E3	1.35E3	5.0E2	2.0E2	6.5E1	1.7E1	3.5E0
	+2	2.1E3	1.05E3	5.0E2	1.9E2	7.0E1	2.2E1	6.7E0	1.7E0
-100	-2	3.3E4	3.2E4	3.10E4	3.0E4	2.9E4	2.6E4	2.4E4	2.1E4
	-1	3.1E4	2.9E4	2.8E4	2.5E4	2.2E4	1.9E4	1.7E4	1.2E4
	0	2.7E4	2.5E4	2.1E4	1.9E4	1.4E4	1.1E4	5.5E3	2.3E3
	+1	2.2E4	1.9E4	1.3E4	9.0E3	6.0E3	3.2E3	1.6E3	7.0E2
	+2	1.5E4	1.0E4	6.1E3	4.9E3	2.4E3	1.1E3	5.0E2	1.9E2

Figure 3. Comparison of stiffness of asphalt obtained manually from nomograph and stiffness of asphalt predicted from regression Eq. 8.

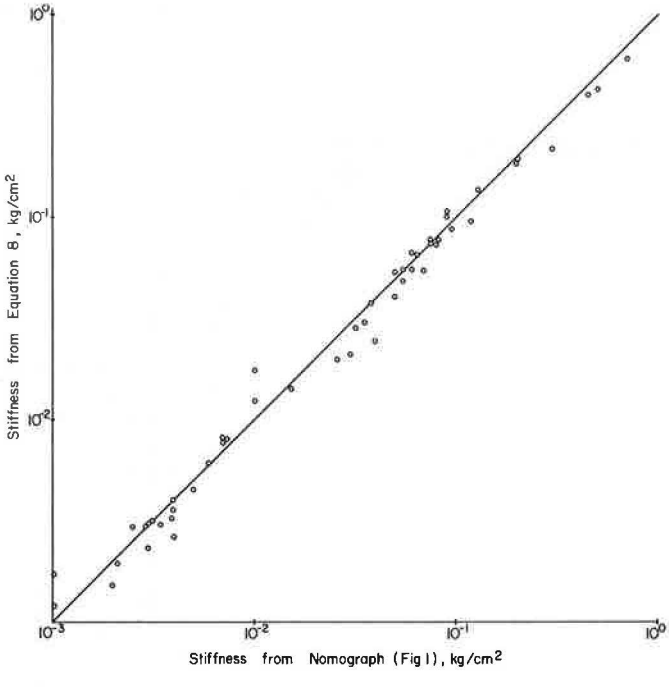

Figure 4. Comparison of stiffness of asphalt obtained manually from nomograph and stiffness of asphalt predicted from regression Eq. 9.

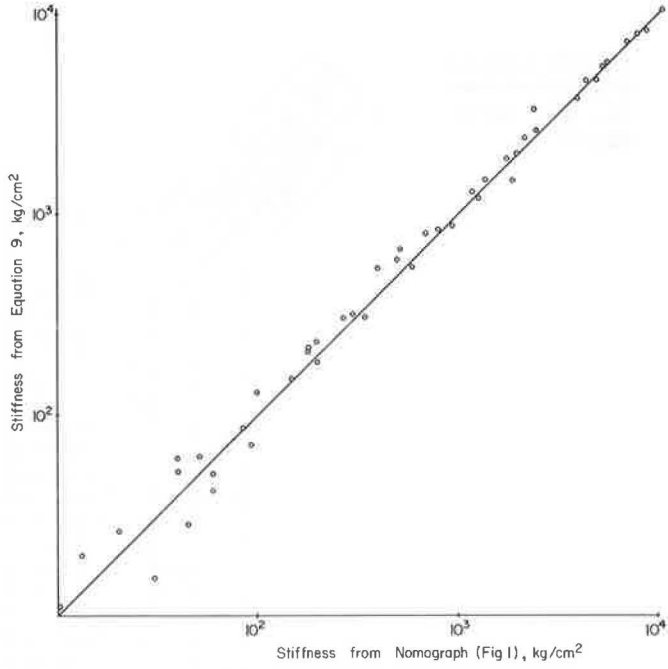

Table 1. Asphalt concrete mixture properties.

Property	Value
Recovered penetration at 77 F, 100 grams, 5 sec	31[a]
Recovered softening point, ring and ball, deg F	132[a]
Percentage of asphalt by weight of aggregate	5.1
Average density of the compacted specimens, lb/ft³	152
Average thermal coefficient of contraction, deg F	1.35×10^{-5}

[a]Estimated.

Figure 5. Measured and assumed asphalt concrete specimen temperatures for thermal stress calculations.

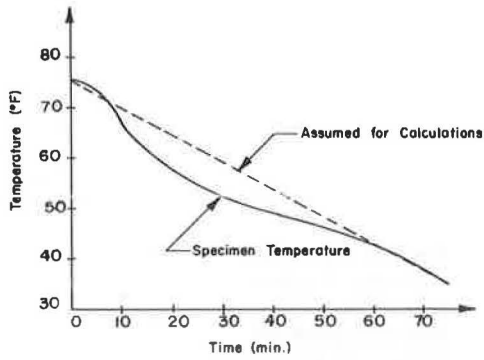

Figure 6. Calculated thermal stresses (in psi).

(Temperature drop 75-35°F, period of 4500 seconds)

Temperature Interval, °F \ Loading Time, seconds	10	100	1000
.04	96.51	34.02	7.18
.4	96.43	34.08	7.25
4.0	96.67	33.55	7.42
5.0	95.72	32.94	7.91
8.0	95.95	33.19	4.91
10.0	94.61	34.66	4.81
20.0	93.16	32.54	4.11
40.0	75.73	11.06	2.37

$$\sigma = \alpha \sum_{T_o}^{T_f} \Delta T \times S(t, \overline{T}_\Delta) \qquad (8)$$

where

α = average coefficient of thermal contraction over the temperature range;
$S(t, \overline{T}_\Delta)$ = stiffness modulus, at the midpoint of the temperature interval ΔT and a loading time t; and
T_o and T_f = initial and final temperatures of the temperature drop.

Figure 7 shows the results of the calculations. The figure seems to indicate the following conclusions:

1. A temperature interval as large as 20 F will result in an acceptable approximation, and
2. The choice of the appropriate loading time is more important than the temperature interval.

Because of the preceding conclusions, a more rational approach for estimating the actual thermal loading time was developed and is summarized as follows:

1. Estimate the average rate of daily pavement temperature drop from U.S. Weather Bureau reports.
2. Experimentally determine the developed thermal stresses in an asphalt concrete beam in a reasonable period of time by subjecting it to the rate of temperature drop estimated in step 1. This can be performed by putting the asphalt concrete beam in an environmental chamber in the laboratory and using the technique described by Monismith et al. (8) or Tuckett et al. (10) or any similar technique.
3. Calculate the developed thermal stress for the same temperature conditions (step 2) by using different loading times.
4. Plot the relation between the loading time and the corresponding thermal stress for the tested asphalt concrete mixture.
5. Find the actual thermal loading time by locating the measured thermal stress (step 2) on the graph (step 4).

The application of the method for the previous example is shown in Figure 8. The thermal stresses were calculated for different loading times at a temperature interval of 4 F. The measured thermal stress, 27.5 psi, was found on the vertical axis, and the actual loading time was estimated as 155 sec. By using this value of loading time, a comparison was made between the calculated and measured thermal stresses (Fig. 9).

In the same figure, the thermal stresses calculated by the conventional method $\left(\text{loading time} = \frac{\text{total time}}{\text{number of intervals}} = 450 \text{ sec}\right)$ are shown.

Figure 9 shows the following:

1. When the difference between the assumed and the actual specimen temperatures is recognized, it is obvious that the agreement between the measured and calculated thermal stresses (based on the proposed method for estimating the thermal loading time) is good. At the beginning of the test, where the actual rate of temperature drop was higher than the assumed value, the observed rate of thermal stresses buildup was also higher than the calculated rate. However, at the end of the test, the reverse was true.
2. The maximum thermal stress calculated by the conventional method is almost half the measured value in this example.

Generally speaking, the conventional method can predict different values of thermal stresses depending on the engineering judgment in choosing the size of the temperature interval.

Figure 7. Maximum thermal stresses for a linear temperature drop of 75 to 35 F in 4,500 sec.

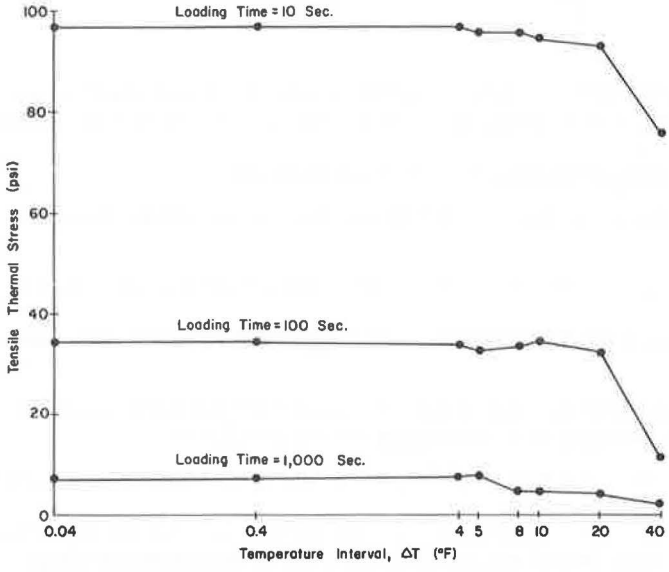

Figure 8. Estimation of the actual thermal loading time.

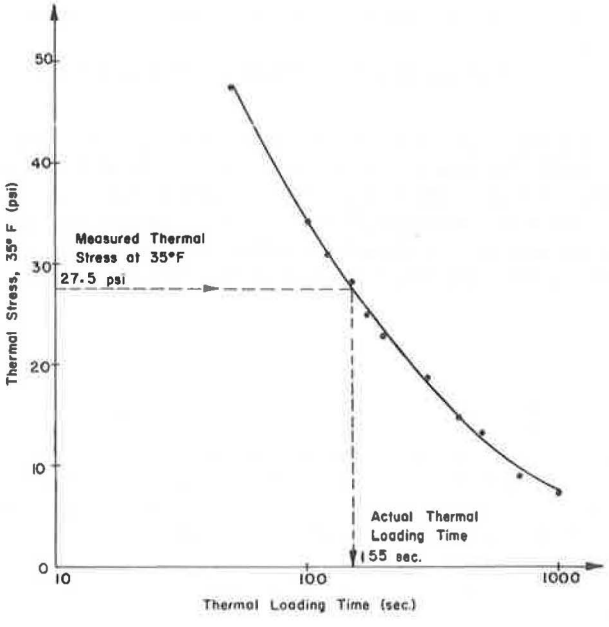

IN-SERVICE AGING OF ASPHALTS

In the previous sections, a model was developed to estimate the stiffness of asphalt, knowing its penetration and softening point. In this section, the history of penetration and softening point is investigated, and models to estimate the aging effect are developed. The intention is to use these models in conjunction with the asphalt stiffness model to estimate the stiffness of asphalt concrete mixtures as a function of temperature, loading time, and age.

Sources of Data Used in Developing the Asphalt Aging Models

In developing the models, a stepwise regression computer program (11) was used. An extensive search was conducted for projects all over the United States where asphalt hardening studies had been conducted. The data from these projects were difficult to correlate and use because different asphalt properties were measured at each one. The locations and the references used in developing the penetration and the softening-point aging models are as follows:

1. Penetration—California (8, 12, 13, 14), Delaware (15), Utah (16, 17), and Pennsylvania (18); and
2. Softening point—California (8, 12, 13, 14) and Delaware (15).

Penetration Aging Model

The purpose of developing the model is to predict the penetration of the in-service asphalt (at any time after construction) from the ordinary laboratory measurements. An acceptable prediction equation was obtained using the stepwise regression technique. The following is the equation with the corresponding statistics:

$$\text{Pen (time)} = -48.258 - 2.561\sqrt{\text{TIME}} + 0.1438\ (\text{OPEN}) - 8.466\ (\text{VOID})\ (\text{XTIME}) + 1.363\ (\text{TFOT}) + 0.9225\ (\text{OPEN})\ (\text{XTIME}) \quad (8)$$

where

time = time placement of the asphalt concrete mixture, months;
XTIME = $1/(\sqrt{\text{TIME}} + 1)$;
OPEN = original penetration, 100 grams, 5 sec, 77 F;
VOID = initial percentage of voids in the asphalt concrete mixture (preferably after mixture placement and compaction); and
TFOT = thin-film oven test, percentage of original penetration.

The corresponding statistics are number of cases, 93; number of variables in the model, 5; mean of the dependent variable (penetration), 49.5; standard error for residuals, 13.1; coefficient of variation, 26.51 percent; multiple R, 0.922; and multiple R^2, 0.85.

This model is valid only for the following ranges of the different variables: time, 1 to 100 months; original penetration, 60 to 240; percentage of voids, 3.8 to 13.6; and TFOT (original penetration < 100), 55 to 70 percent; (original penetration 100 to 175), 45 to 70 percent; and (original penetration > 175), 30 to 70 percent.

The model explains 85 percent of the variability of the dependent variable (penetration).

Also, the model shows a coefficient of variation of 26.5 percent. This value resulted not only from a lack of fit but also from unexplained errors (measured errors, human variations, replications, etc.). Welborn (19) reported that, in some projects where the mean penetration was 46.7, the standard deviation reached 17.6, which gives a coefficient of variation of about 38 percent.

Figure 10 shows the relation between estimated and measured values of penetration for the 93 cases used to predict the model. The effect of the variation of each of the individual factors in the model (Eq. 8) is discussed in the following paragraphs.

With both the initial voids (9 percent) and the TFOT (60 percent) as constants, Figure 11 shows the decrease of penetration with time for five different original penetration values. From the figure, the following observations can be made:

Figure 9. Comparison between measured and estimated tensile thermal stresses.

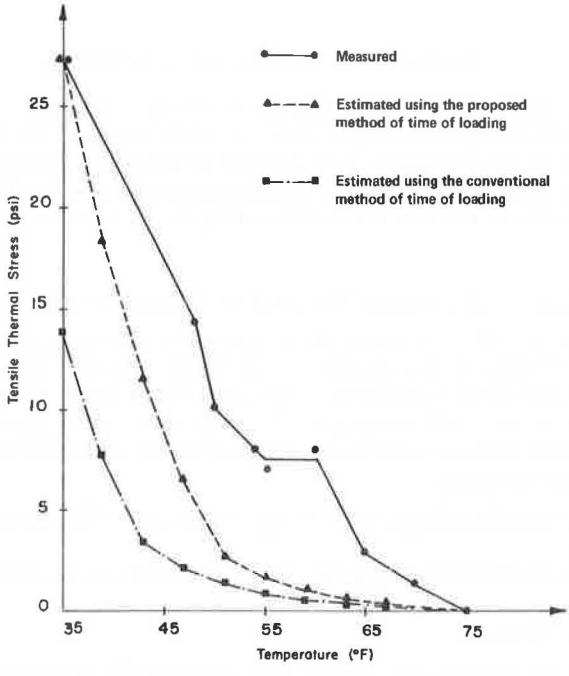

Figure 10. Measured in-service penetration versus predicted values from the penetration model.

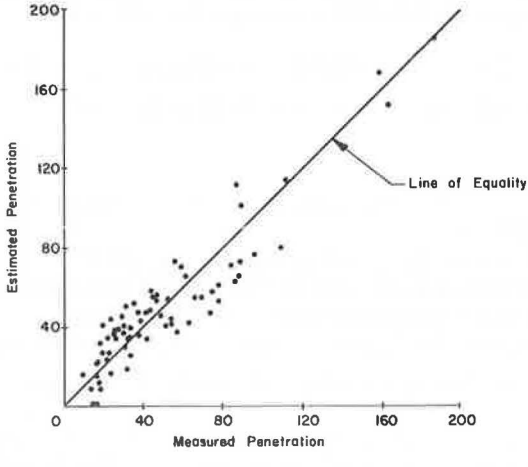

Figure 11. Effect of original penetration on in-service values of penetration as predicted from penetration model.

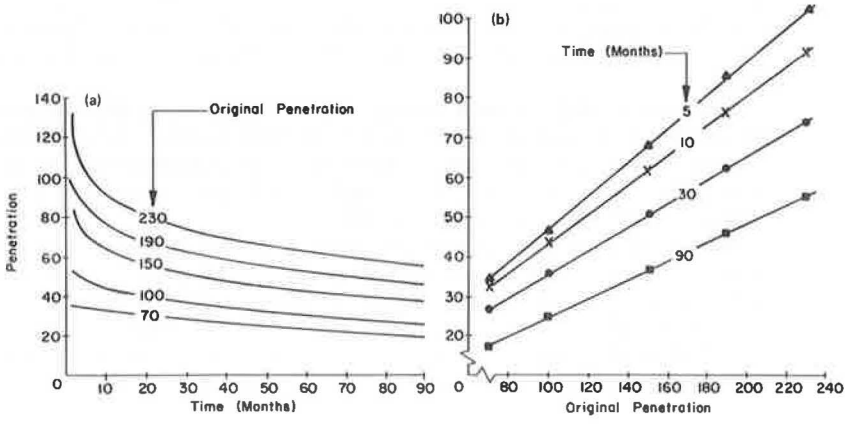

1. The higher the original penetration is, the higher the rate of initial hardening (Fig. 11a) is;
2. The rate of hardening decreases considerably with time for all values of original penetration (Fig. 11a); and
3. The penetration at a given time is a linear function of the original penetration (Fig. 11b).

Based on an original penetration of 100 and a TFOT of 60 percent, Figure 12 shows the effect of five levels of voids on asphalt hardening. The higher the percentage of voids is in the asphalt concrete mixture, the higher is the hardening of the asphalt. Vallerga and Halstead (20) concluded the following: "In pavements of below 2 percent voids, field aging during 11 to 13 years appeared to have been negligible. Above this level, hardening increased with air voids."

Field observations have shown a direct correlation between the percentage of original penetration from the TFOT and the percentage of original penetration after field mixing. In addition, laboratory results from different asphalts have shown that the higher the original penetration is, the lower the percentage of original penetration after the TFOT is. Therefore, the developed penetration model was used to analyze the behavior of two different asphalts having different original penetrations under different TFOT percentages (Fig. 13). As expected, more hardening occurred during the mixing process for asphalts exhibiting a lower percentage of original penetration after the TFOT.

Softening-Point Aging Model

The purpose of this model is to predict the softening point of the in-service asphalt (any time after construction) from the ordinary laboratory measurements. An acceptable prediction equation was obtained using the stepwise regression technique. The following is the equation with the corresponding statistics:

$$TRB\ (TIME) = -4.632 + 3.162\ TIME + 1.585\ (ORB) - 0.93\ (TFOT) \qquad (9)$$

where

TIME = time from placement of the asphalt concrete mixture, months;
ORB = original ring and ball temperature, deg F; and
TFOT = thin-film oven test, percentage of original penetration.

The corresponding statistics are number of cases, 49; number of variables in the model, 3; mean of the dependent variable, 134.4; standard error for residuals, 4.8; coefficient of variation, 3.6 percent; multiple R, 0.93; and multiple R^2, 0.87.

This model is valid only for the following ranges of the different variables: time, 1 to 100 months; original ring and ball temperature, 99 to 125 F; and TFOT, 30 to 70 percent.

With only three variables in the model, the multiple $R^2 = 0.87$ indicates that the model is satisfactory. It can be seen that the voids did not enter the final model, which can be explained by the fact that the 49 cases have percentages of voids that are relatively high.

A plot of measured versus estimated values of the softening point for the 49 cases used to predict the model is shown in Figure 14.

The behavior of the model for different values of each factor in the mathematical equation was studied by programming the model and varying the factors one at a time with the others held constant. Figure 15 shows the increase of softening point with time for three different original softening points (100, 110, and 120 F) and a constant value of TFOT (60 percent).

Figure 16 shows the same concept for three different values of TFOT (40, 50, and 60 percent) and a constant initial softening point (110 F).

Factors Considered But Not Used in the Final Models

For different reasons, several variables were considered but not used in the final models (Eqs. 8 and 9).

Climatography Factors—The following factors were considered: solar radiation on

Figure 12. Effect of five levels of voids on asphalt hardening.

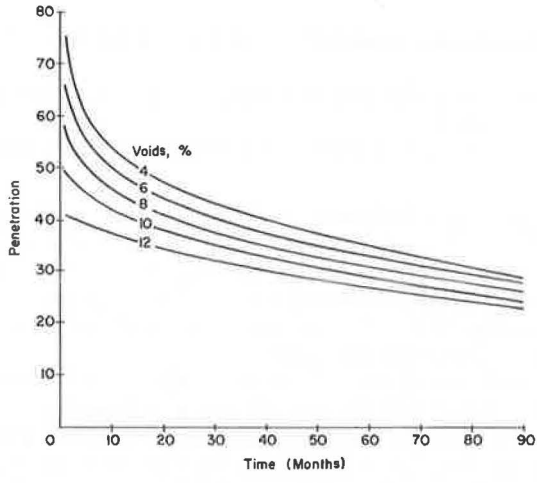

Figure 13. Effect of TFOT on in-service values of penetration as predicted from penetration model.

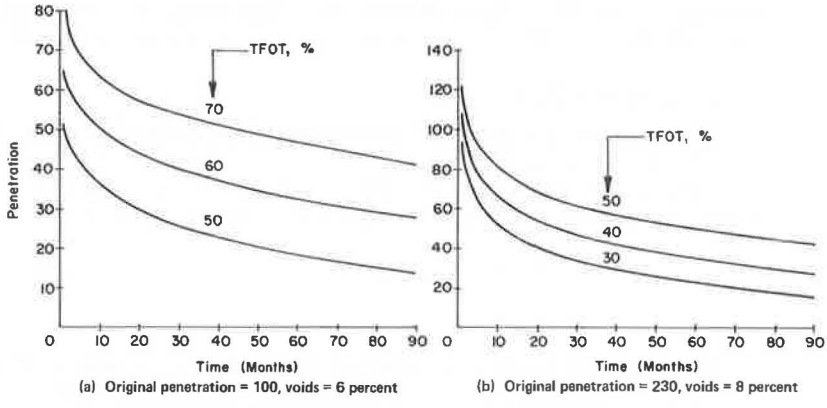

Figure 14. Measured in-service softening point versus predicted values from the softening-point model.

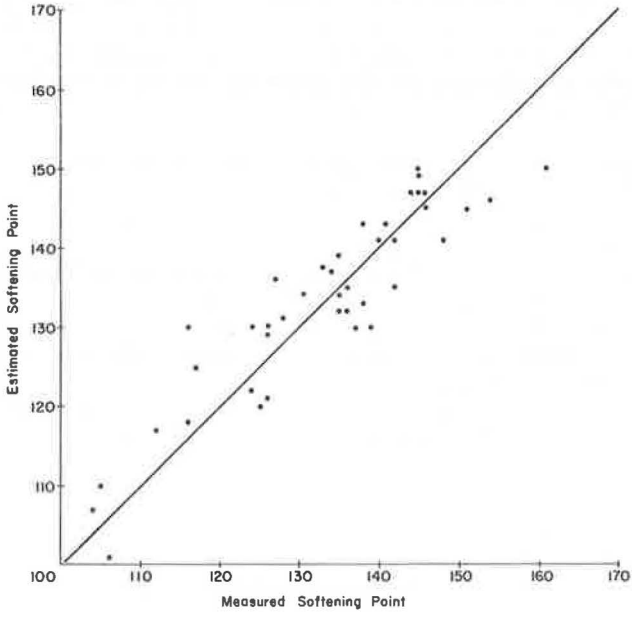

annual basis, wind velocity, number of days > 90 F, average annual temperature, and average annual daily range of temperatures.

The most significant environmental variable that showed a high correlation with asphalt hardening was the solar radiation. However, because of the limited number of geographical locations, it was decided not to include it in the final models, but it should be considered in future investigations.

Inverse Gas-Liquid Chromatography—IGLC is a new technique developed by Davis et al. (21). In this test, the asphalt is absorbed on the surface of an inert support and placed in a chromatography column. Different chemical test compounds are injected individually into the column. Based on the retention time for a nonreactive material of the same molecular weight as the test compound, a parameter known as the interaction coefficient (Ip) is computed. The higher the value of Ip is, the higher is the reaction of the test compound with the asphalt. An extension of this technique was introduced by Davis and Peterson (22). The extension suggests the oxidation of the asphalt in the chromatography column before injecting the chemical test compounds.

In developing both asphalt hardening models (penetration and softening point), Ip resulting from injecting phenol into oxidized asphalt showed extremely high correlation with asphalt hardening. The IGLC test values were not included in the final aging models because of the shortage of test locations where the test was performed. The IGLC is believed to hold a promise for improved prediction of asphalt hardening and thus should be given attention in future research studies.

Asphalt Components—The five components of asphalt are asphaltness A, nitrogen bases N, first "acidaffins" A1, second acidaffins A2, and paraffins P. The ratio $(N + A1)/(P + A2)$ was proposed by Rostler to express the ratio between more reactive components to the less reactive ones. None of the variables showed a significant correlation with asphalt hardening (penetration and softening point). Gotolski et al. (18) concluded the following about asphalt components: "In the overall picture, the asphaltene content or that of any of the other single components does not determine the performance of asphalts."

Percentage of Asphalt—The percentage of asphalt in the asphalt concrete mixture showed a correlation with asphalt hardening whenever it was considered without considering the effect of the percentage of air voids in the mixture. However, whenever the percentage of voids enters the models, the percentage of asphalt loses its significance. This is logical because the percentage of voids and percentage of asphalt are known to be related to each other.

Asphalt Viscosity—Viscosity is not included in final aging models because asphalt viscosities were determined under different conditions for all the projects used to develop the models, and it was difficult to match the viscosity results from all the projects. A specific viscosity test and test conditions should be established and specified for future studies.

Penetration Index—The penetration index suggested by Pfeiffer and Van Doormaal (23) correlated with asphalt hardening. However, because of the limited range of the penetration indexes reported in the different projects, this factor was omitted from the final models.

PREDICTION OF ASPHALT CONCRETE STIFFNESS

The usefulness of the system can be shown by estimating the asphalt concrete stiffness at the normal monthly average air temperatures, for a period of 5 years (starting from the month of July), for the cities of El Paso and Los Angeles. It should be noted that using the air temperature for the calculations is misleading because the asphalt concrete temperature is different from the air temperature (1). However, the purpose of this example is to illustrate the use of the system only.

The asphalt concrete properties and loading time used for the calculations are given in Table 2. The normal monthly average air temperatures for the cities of El Paso and Los Angeles are given in Table 3. Figure 17 shows the results of the calculations, from which one may conclude the following:

1. There is a sudden increase in the modulus during the first month, mainly because

Figure 15. Effect of original softening point on in-service values of softening point as predicted from softening-point model.

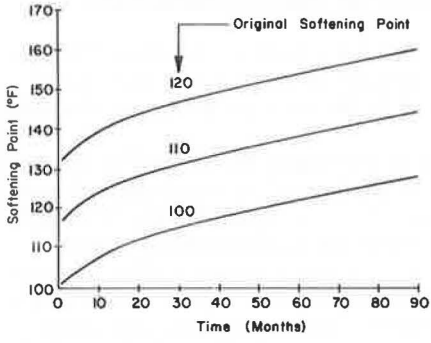

Figure 16. Effect of TFOT on in-service values of softening point as predicted from softening-point model.

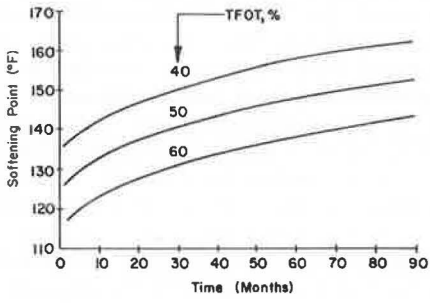

Table 2. Assumed asphalt concrete mixture properties and loading times.

Property	Value
Original penetration at 77 F, 100 grams, 5 sec	95
Original softening point, deg F	115
Percentage of original penetration after TFOT	60
Percentage of air voids	5
Volume of concentration of the aggregate	0.87
Time of loading, sec	100

Table 3. Normal monthly average temperatures.

City	July	Aug.	Sept.	Oct.	Nov.	Dec.	Jan.	Feb.	Mar.	April	May	June
El Paso	81.9	80.4	74.5	64.4	51.2	44.1	42.9	49.1	54.9	63.4	71.9	81.0
Los Angeles	69.1	69.1	68.5	64.9	61.6	56.9	54.4	55.2	57.0	59.4	62.0	64.8

Figure 17. Example of the variation of the monthly average asphalt concrete stiffness as estimated from the system.

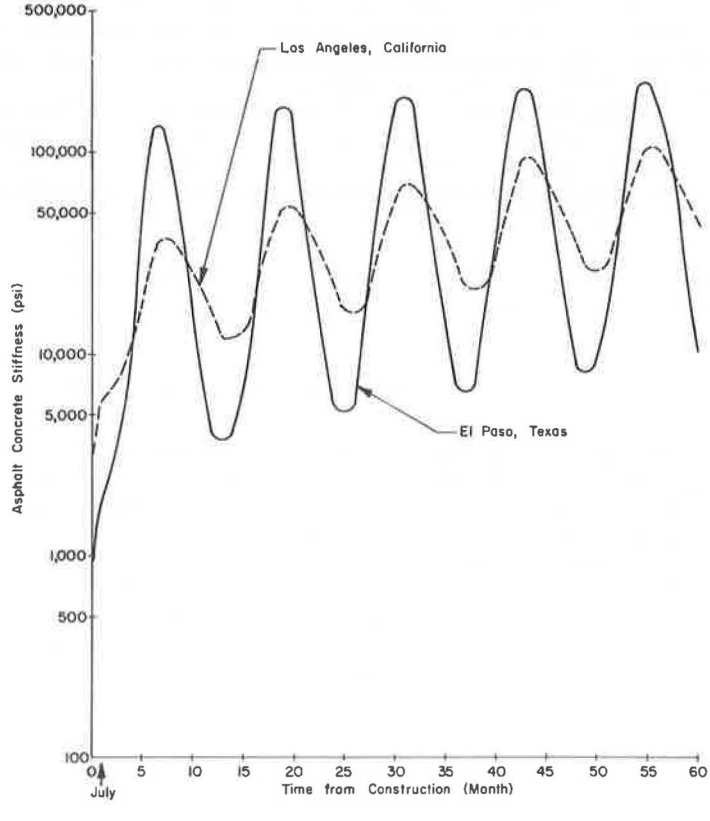

of the hardening of asphalt that occurs during the mixing process;

2. The range of the annual stiffness variation is different among locations, depending on the annual temperature range;

3. Considering a single stiffness value for the purpose of design of an asphalt concrete surface is inadequate;

4. Because low stiffness is the most critical for traffic loads, the asphalt concrete stiffness during the first July after construction is the one to be considered; and

5. Because high stiffness is the most critical for temperature, the asphalt concrete stiffnesses during December and January, several years from construction, are the ones to be considered.

SUMMARY AND RECOMMENDATIONS

In this research effort, a system for predicting asphalt concrete stiffness history has been developed. The main constituents of the system are the asphalt concrete stiffness and aging models. The objective of the system is to help analyze the different modes of distress in asphalt concrete surfaces. The system has been utilized in predicting low-temperature and thermal-fatigue cracking due to daily temperature cycling (1), and it has shown a good degree of reliability.

In addition, it is recommended that the system be used in conducting the following studies:

1. The establishment of a rational specification for asphalt concrete mixture design,

2. The provision of a tool to differentiate among the different asphalt sources in a particular location, and

3. The advancement of the fatigue distress studies due to traffic loads (24).

ACKNOWLEDGMENTS

This investigation was conducted at the Center for Highway Research, University of Texas at Austin. The authors wish to thank the sponsors, the Texas Highway Department and the Federal Highway Administration, U.S. Department of Transportation.

The contents of this report reflect the views of the authors, who are responsible for the facts and the accuracy of the data presented herein. The contents do not necessarily reflect the official views or policies of the Federal Highway Administration. This report does not constitute a standard, specification, or regulation.

REFERENCES

1. Shahin, M. Y. Prediction of Low-Temperature and Thermal-Fatigue Cracking in Flexible Pavements. Univ. of Texas at Austin, PhD dissertation, Aug. 1972.
2. Van der Poel, C. A General System Describing the Viscoelastic Properties of Bitumens and Its Relation to Routine Test Data. Jour. of Applied Chemistry, Vol. 4, May 1954.
3. Pell, P. S., and McCarthy, P. F. Amplitude Effect of Stiffness of Bitumen and Bituminous Mixes Under Dynamic Conditions. Rheologia Acta, Vol. 2, No. 2, 1962.
4. Monismith, C. L. Asphalt Mixture Behavior in Repeated Flexure. Univ. of California, Berkeley, IER Rept. TE-65-9, Nov. 1965.
5. Heukelom, W., and Klomp, A. J. G. Road Design and Dynamic Loading. Proc., AAPT, Vol. 33, Feb. 1964, pp. 92-125.
6. Van Draat, W. E. F., and Sommer, P. Ein Gerat zur Bestimmung der Dynamischen Elastizitattsmoduln von Asphalt. Strasse und Autobahn, Vol. 35, 1966.
7. Draper, N. R., and Smith, H. Applied Regression Analysis. John Wiley and Sons, New York, 1966.
8. Monismith, C. L., Secor, G. A., and Secor, K. E. Temperature Induced Stresses and Deformations in Asphalt Concrete. Proc., AAPT, Vol. 34, Feb. 1965, p. 248.
9. Hills, J. F., and Brien, D. The Fracture of Bitumens and Asphalt Mixes by Temperature Induced Stesses. Proc., AAPT, Vol. 35, Feb. 1966, p. 292.
10. Tuckett, G. M., Jones, G. M., and Littlefield, G. The Effects of Mixture Variables

on Thermally Induced Stresses in Asphaltic Concrete. Proc., AAPT, Vol. 39, Feb. 1970, p. 703.
11. STEP-01: Statistical Computer Program for Stepwise Multiple Regression. Center for Highway Research, Univ. of Texas at Austin, 1968.
12. Hveem, F. N., Zube, E., and Skog, J. Progress Report on the Zaca-Wigmore Experimental Asphalt Test Project. Symposium on Paving Materials, ASTM, Spec. Tech. Publ. 277, 1959, pp. 3-45.
13. Skog, J. Results of Cooperative Test Series on Asphalts From the Zaca-Wigmore Experimental Project. Symposium on Paving Materials, ASTM, Spec. Tech. Publ. 277, 1959, pp. 46-51.
14. Zube, E., and Skog, J. Final Report on the Zaca-Wigmore Asphalt Test Road. Presented to Materials and Research Dept., California Division of Highways, 1959.
15. Kenis, W. J., Sr. Progress Report on Changes in Asphaltic Concrete in Service. HRB Bull. 333, 1962, pp. 39-65.
16. Beteson, W. B. Rubber in Asphalt, Field and Laboratory Performance Testing. Internat. Symposium on the Use of Rubber in Asphalt Pavements, Salt Lake City, May 1971.
17. Liddle, W. J., Jones, G. M., Peterson, D. E. Use of Synthetic Rubber-in-Asphalt Pavement to Determine Mixture Behavior and Pavement Performance. Materials and Tests Div., Utah State Highway Department, Interim Rept., Dec. 1969.
18. Gotolski, W. H., Ciesielski, S. K., and Heagy, L. N. Progress Report on Changing Asphalt Properties of In-Service Pavements in Pennsylvania. Proc., AAPT, Vol. 33, Feb. 1964, pp. 285-319.
19. Welborn, J. Y. Asphalt Hardening: Fact and Fallacy. Public Roads, Vol. 35, No. 12, Feb. 1970, pp. 279-285.
20. Vallerga, B. A., and Halstead, W. J. Effects of Field Aging on Fundamental Properties of Paving Asphalts. Highway Research Record 361, 1971, pp. 71-92.
21. Davis, T. C., Peterson, J. C., and Haines, W. E. Inverse Gas-Liquid Chromatography: A New Approach for Studying Petroleum Asphalts. Analytical Chemistry, Vol. 38, No. 2, Feb. 1966, pp. 241-243.
22. Davis, T. C., and Peterson, J. C. An Adaptation of Inverse Gas-Liquid Chromatography to Asphalt Oxidation Studies. Analytical Chemistry, Vol. 38, No. 13, Dec. 1966, pp. 1938-1940.
23. Pfeiffer, J. P., and Van Doormaal, P. M. The Rheological Properties of Asphaltic Bitumen. Jour. Institute of Petroleum Technology, Vol. 22, 1936.
24. Jain, S. P., McCullough, B. F., and Hudson, W. R. Flexible Pavement System—Second Generation, Incorporating Fatigue and Stochastic Concepts. Texas Highway Department; Texas Transportation Institute, Texas A&M Univ.; and Center for Highway Research, Univ. of Texas at Austin, Res. Rept. 123-10, Dec. 1971.